Recent Changes in Downward Longwave Radiation at King Sejong Station, Antarctica

HI KU CHO, JHOON KIM, YEONJIN JUNG, AND YUN GON LEE

Global Environment Laboratory/Department of Atmospheric Sciences, Yonsei University, Seoul, South Korea

BANG YONG LEE

Korea Polar Research Institute, KORDI, Inchun, South Korea

(Manuscript received 1 February 2007, in final form 19 March 2008)

ABSTRACT

Effects of cloud, air temperature, and specific humidity on downward longwave irradiance and their long-term variabilities are examined by analyzing the measurements made at the King Sejong Station in the Antarctic Peninsula during the period of 1996–2006.

It has been shown that the downward longwave irradiance (DLR) is significantly correlated with three variables: air temperature, specific humidity, and cloudiness. Based on the relationship of the three variables with DLR, a multiple linear regression model has been developed in order to evaluate the relative contribution of each of the variables to the variation of DLR. The three variables together explained 75% of all the variance in daily mean DLR. The respective contribution from specific humidity and cloudiness to the variation of DLR was 46% and 23%; thus most of the DLR variability can be explained by the variations in the two variables. The annual mean of longwave cloud forcing shows 52 W m^{-2} with no remarkable seasonal cycle. It is also noted that the overcast cloud effect gives an increase by 65 W m^{-2} with respect to clear-sky flux throughout the year. It is suggested that the multiple regression model can be used to estimate the radiative forcings of variables influencing the DLR variability.

A highly significant decrease in DLR with an average of -1.52 W m^{-2} yr^{-1} (-0.54% yr^{-1}) is found in an analysis from the time series of the deseasonalized monthly mean values. Accordingly, the atmospheric flux emissivity, air temperature, and specific humidity have also decreased in their time series, while the cloudiness has increased insignificantly. Consequently, it may be concluded that the recent decrease in DLR is mainly attributed to the net cooling effect due to the decrease in air temperature and specific humidity, which overwhelm the slight warming effect in cloudiness. Analysis of mean monthly trends for individual months shows that, as for the annual data, the variations in DLR are mostly associated with those of air temperature, specific humidity, and cloudiness.

1. Introduction

Downward longwave radiation is one of the key components in the energy balance for the earth–atmosphere system. Polar regions play a critical role in the surface energy balance and climate system of the earth. Recently, one of the important questions regarding these regions concerns the role of the Antarctic atmospheric heat sink in global climate (Studinger et al. 2005). For scientific research and observation in the earth's polar regions, the International Polar Year (IPY), 2007–08, was initiated by the International Council for Science (ICSU) and the World Meteorological Organization (WMO 2007). In recent years much attention has been given to studying the surface energy balance (e.g., Schlatter 1972; King et al. 1996; Reijmer and Oerlemans 2002; van den Broeke et al. 2004; Kim et al. 2006) and the long-term trends in solar irradiance, cloudiness, and surface air temperature (e.g., Dutton et al. 1991; Stanhill and Cohen 1997) in Antarctica. On the other hand, Dutton et al. showed that the solar irradiance at the South Pole unexpectedly showed a statistically significant decrease between 1976 and 1987 during the late austral summer season, where seasonally increasing cloud cover is directly associated with decreasing solar irradiance trends. According to Stanhill and Cohen, solar irradiance in Antarctica

Corresponding author address: Jhoon Kim, Global Environment Laboratory/Department of Atmospheric Sciences, 134 Sinchon-dong, Seodaemoon-gu, Seoul 120-749, South Korea.
E-mail: jkim2@yonsei.ac.kr

DOI: 10.1175/2008JCLI1876.1

showed a highly significant decrease during the last 39 years. They noted that the cause of this decrease is not clear but is unlikely due to an increase in the cloud amount because of the changes to surface reflectivity conditions over Antarctica. WMO (2007) reported that temperatures at the South Pole have dropped since the 1950s but there have been no significant changes at the Vostok station. It is shown that the Antarctic Peninsula has experienced a remarkable warming and retreat of ice shelves (King 1994; Vaughan and Doake 1996; Lee et al. 2002; Hodgson et al. 2006; WMO 2007).

Most of the studies referenced above apply to coastal or inland Antarctic sites located at latitudes higher than 65°S. Therefore, for the region of the Antarctic circumpolar trough at lower latitudes, little is known about the overall energy balance or the variability of long-term solar and downward longwave irradiance at the surface together with air temperature, humidity, and cloudiness. This study aims to elucidate the long-term variability in the downward longwave irradiance (DLR) measured during the period from 1996 to 2006 at the Korean King Sejong Station (62.13°S, 58.47°W; 9.8 m MSL) located at the latitudes of the Antarctic circumpolar trough, Fig. 1. To understand the long-term variability of DLR, it is necessary to examine the effects of air temperature, specific humidity, and cloudiness on the DLR.

2. Climate

The King Sejong Station is located on the Barton Peninsula of King George Island, one of the South Shetland Islands off the northern tip of the Antarctic Peninsula. The station was established in 1988 and has provided meteorological records to monitor and understand the meteorological environment of King George Island. Also, as one of the WMO Antarctic Basic Synoptic Network (WMO Index No. 89251), the station has monitored variations of the Antarctic climate since 1988. For the austral summer season (December–February), the surface air temperature is above freezing and surface winds exhibit mostly northwesterlies. On the other hand, strong southeasterly winds predominate in the austral winter season (June–August), and these are frequently accompanied by severe blizzards. The severe weather phenomena are caused by remarkable pressure patterns in the Antarctic circumpolar trough and topographical effects at the King Sejong Station. The climate around the station is affected mostly by the polar lows in the trough throughout the year. The climatological data (1988–2006) is summarized in Table 1.

The King Sejong Station exhibits relatively warm and wet conditions compared with those of inland stations in Antarctica, which shows the characteristics of an oceanic climate in the polar region. As can be seen in Table 1, the annual mean values over the 1988–2006 period are −1.6°C for surface air temperature, 8.0 m s^{-1} (up to the extreme value of 46.6 m s^{-1}) for surface wind speed, about 89% for relative humidity and 6.7 oktas for cloud cover. In particular, approximately one out of three days is in overcast conditions at King Sejong Station. No remarkable seasonal variations for relative humidity and cloudiness are observed.

3. Instrumentation and data acquisition

The downward component of longwave irradiance has been measured since 1996 using an Eppley Precision Infrared Radiometer (PIR; pyrgeometer) mounted 1.8 m above the ground surface. The Eppley pyrgeometer consists of a thermopile detector covered by a silicon hemisphere that is transparent for far-infrared radiation (spectral range 4–50 μm) but absorbs solar radiation. Eppley recommends a minimum calibration cycle of 5 yr but encourages annual calibrations for reliable measurements with consistent accuracy (Eppley 2006). Two Eppley Precision Infrared pyrgeometers (Model PIR serial numbers 30967F3 and 32689F3) are available for measuring DLR at King Sejong Station. These PIR detectors have been calibrated with the Eppley standard detectors by sending them one at a time to the manufacturer. During the calibration process of one detector, measurements are taken with the other detector. As shown in Table 2, PIR calibrations have been alternately carried out after four years (first phase, 1995–99), then again after two years (second phase, 1999–2001), and every year since 2001 (third phase). A statistical analysis of an ensemble of the calibrations of the instrument taken over the last 11 years yields the standard deviations of 2.1% for PIR number 30967F3 and 2.3% for PIR number 32689F3, which do not include any systematic errors in the Eppley procedure. Each pyrgeometer has been compared at Eppley against their Blackbody Calibration System under radiation intensities of approximately 200 W m^{-2} and an average ambient temperature of 25°C as measured by a Standard Omega Temperature Probe, Resistance Temperature Detector (RTD) number 1. As a result of a series of comparisons, the PIR detector has been found to have an approximate mean sensitivity of 4.0×10^{-6} V (W m^{-2}) $^{-1}$. The calculation of this constant is based on the fact that the relationship between radiation intensity and emf is rectilinear to intensities of 700 W m^{-2}, and the radiometer is linear to within ±1.0% up to this intensity.

The PIRs have been inspected by an observer everyday, keeping the dome clear by using a soft cloth or

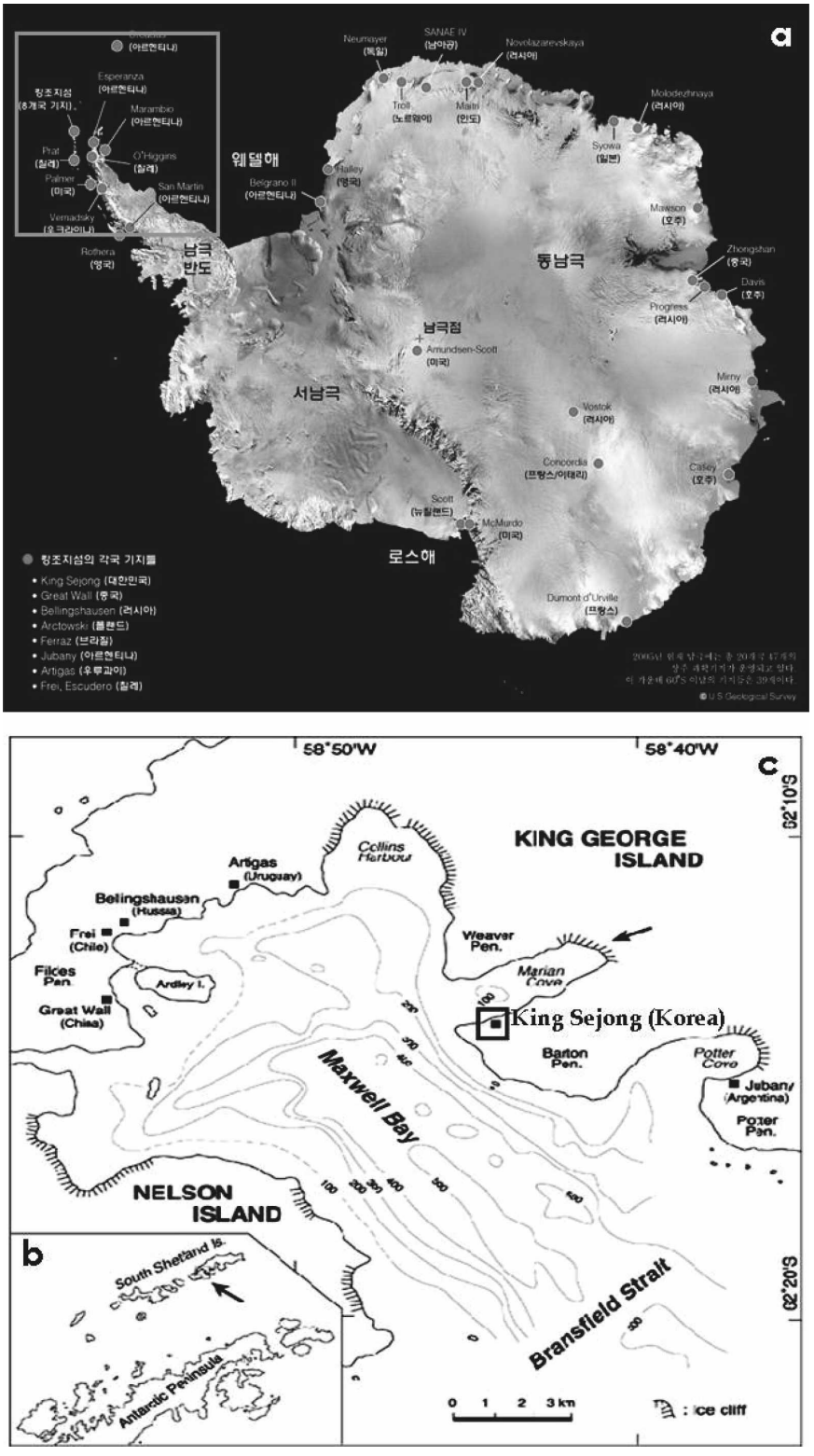

FIG. 1. (a) Antarctica, (b) the Antarctic Peninsula, and (c) the location of King Sejong Station (62°13′S, 58°47′W, 9.8 m MSL) on King George Island.

TABLE 1. Climate summary of seasonal mean solar irradiance, longwave irradiance, and meteorological data at King Sejong station (1988–2006). Number in parenthesis is the standard deviation. Total UV is from the Eppley UV photometer (295–385 nm); UV-A is from the Solar Light UV-meter (320–400 nm); EUV is erythermal UV from the Solar Light UV-Biometer (280–320 nm).

Component	Spring (SON)	Summer (DJF)	Autumn (MAM)	Winter (JJA)	Year
Global solar (W m^{-2})	115.0 (38.6)	155.5 (33.4)	39.5 (25.5)	16.5 (10.3)	81.9 (3.5)
Total UV [1994–2006] (W m^{-2})	8.7 (3.5)	10.7 (2.5)	3.1 (1.7)	2.0 (1.6)	5.9 (0.8)
UV-A [2000–2006] (W m^{-2})	1.0 (0.4)	1.2 (0.3)	0.3 (0.2)	0.1 (0.1)	0.6 (0.1)
EUVB$\times 10^{-2}$ [1995–2006] (W m^{-2})	1.8 (0.8)	2.6 (0.8)	0.3 (0.3)	0.1 (0.1)	1.2 (0.2)
Infrared [1996–2006] (W m^{-2})	277.3 (11.5)	295.2 (8.8)	282.1 (12.3)	264.0 (10.9)	279.9 (6.8)
Temperature (°C)	−2.0 (1.9)	1.7 (0.8)	−1.1 (2.2)	−5.1 (2.4)	−1.6 (0.7)
Pressure (hPa)	987.5 (6.0)	988.0 (5.1)	990.3 (4.7)	991.1 (5.4)	989.2 (1.9)
Relative humidity (%)	89.3 (4.2)	88.8 (3.9)	88.7 (4.8)	88.7 (4.2)	88.9 (3.2)
Cloudiness (oktas)	6.7 (0.5)	6.6 (0.4)	6.7 (0.4)	6.9 (0.4)	6.7 (0.3)
Wind speed (m s^{-1})	8.5 (1.2)	7.0 (0.9)	8.0 (0.8)	8.6 (1.0)	8.0 (1.2)
Precipitation (mm)	90.1 (40.6)	146.9 (57.1)	151.5 (61.3)	95.4 (65.9)	484.0 (152.4)

brush. The pyrgeometer remained unshaded during daylight, which at the southern Great Plains site in Oklahoma can lead to, on average, an additional 3 W m^{-2} (Philipona et al. 2001) and 3 $\sim$ −5 W m^{-2} at Tateno, Japan (Ueno et al. 2000) in DLR. Alados-Arboledas et al. (1988) showed that an equivalence of about 3.6% of the solar flux incident on the pyrgeometer is included in the measurements. According to the results of their experiments, the average addition occurs at a relatively small value of 2.9 W m^{-2} at the King Sejong Station because of lower solar elevation and mostly cloudy sky conditions. Thus, the error produced by solar heating of the dome is about 1% of the DLR. This PIR instrument reports DLR with uncertainties less than 3 $\sim$ 5% (T. Kirk 2007, personal communication; Eppley 2006; Fairall et al. 1998) as the dome temperature is not measured. Each radiation component was sampled every 10 s, and 10-min averaged values were stored in a datalogger, which after quality control were converted into 1-h means. The daily mean irradiance is calculated by averaging the set of daily hourly means, and the monthly mean irradiance is obtained by taking the average of all the daily means. Data quality control procedures were implemented to reject data exceeding a double standard deviation ($\pm 2\sigma$) from the daily means of DLR during the period 1996–2006, and the data contaminated by frost-covered domes and attenuated by blowing snow and blizzards. To assess the accuracy and natural variability of the DLR together with T_a, q, and n, the monthly means, their standard deviations, and standard errors are listed in Table 5. In this study, approximately 15% of the total possible daily data for 11 years is either missing or eliminated through data quality control.

Apart from radiation measurements, the station is equipped with the All Weather Inc. (former name: Weather Tronics and Quality Matirics Inc.; additional information is available online at http://www.allweatherinc.com/) Automated Weather Observing Systems (AWOS) for measuring synoptic meteorological variables. The temperature and humidity sensors are ventilated and shielded from radiation at a height of 1.5 m AGL. Air temperature is measured using a Pt100RTD, and relative humidity with a thin-film capacitor sensor of the 5190 series probes, designed by All Weather Inc. The 5190 probes operate with a DC voltage supply and have a low current draw. The signals from the sensors are converted into two linearized voltage output signals. The accuracy of the 5190 series probes are ±0.2°C for air temperature and ±2% (10%–100%) $\sim$ ±3% (0%–10%) for relative humidity. Several 5190 series probes are provided to replace faulty units immediately. These data were recorded every minute in a datalogger and then the processed for daily and monthly means using methods similar to the radia-

TABLE 2. History of the pyrgeometer calibrations.

Serial number		Date of test	Sensitivity of detector [μV/(W m^{-2})]
PIR 30967F3	Original	17 Nov 1995	3.76
	Second	19 Sep 2001	3.91
	Third	22 Jul 2003	3.93
	Fourth	12 Jul 2005	3.88
	Mean value (S)		3.87
	Std dev (Std)		0.08
	Std/S (%)		2.1
PIR 32689F3	Original	3 Aug 1999	3.82
	Second	29 Jul 2002	4.01
	Third	24 Aug 2004	3.99
	Fourth	7 Aug 2006	4.01
	Mean value (S)		3.96
	Std dev (Std)		0.09
	Std/S (%)		2.3

tion data processing. In addition to the measurements described above, surface synoptic observations including cloud cover are available from the King Sejong Station. Clouds have been observed visually at four times per day by a well-trained observer at the station (in units of eighths of the sky or oktas) following guidelines of the WMO. Most of the data used here consist of daily and monthly mean DLR, air temperature, specific humidity, and cloudiness measured during the period from 1996 to 2006.

4. Results and discussion

a. Effects of air temperature, specific humidity, and cloudiness on the downward longwave radiation

The DLR (or $F^{\downarrow}$) from a layer of the atmosphere at effective radiative temperature (T) containing an absorber pathlength (u) in terms of the graybody (broadband emissivity) approximation (e.g., Liou 2002; Goody and Yung 1989) is given by

$$F^{\downarrow}(u, T) = \sigma T^4 \varepsilon^f(u, T), \tag{1}$$

where ε^f is atmospheric broadband flux emissivity expressed by

$$\varepsilon^f(u, T) = \frac{1}{\sigma T^4} \int_0^{\infty} [1 - \tau_{\upsilon}^f(u, T)] B_{\upsilon}(T)\, d\upsilon \tag{2}$$

in which τ_{υ}^f is monochromatic flux transmittance. In this study, the flux emissivity is calculated from Eq. (1) using the ratio of pyrgeometer measured flux to the σT_a^4, where T_a is air temperature at screen height. Here absorber pathlength means those of the greenhouse gases, H_2O, CO_2, and O_3. One of the most important practical applications of infrared radiative transfer theory in the atmosphere is a calculation of the DLR. The infrared radiative transfer depends on both the local temperature and the efficiency of the absorbers of the radiation. In the presence of clouds, radiative transfer depends on cloud amount and the efficiency with which clouds absorb and reemit longwave radiation as well as on the cloud top and base temperature (e.g., Goody and Yung 1989; Kiehl and Trenberth 1997).

In this study, water vapor (specific humidity) and clouds are considered as infrared absorbers. Water vapor is the most important greenhouse absorber in the atmosphere, in clear sky accounting for 60% of the total contribution of the absorbers to the total greenhouse effect (Kiehl and Trenberth 1997). In the presence of cloud, the DLR values undergo considerable changes with increasing effect (e.g., Kondratyev 1969; Yamanouchi and Kawaguchi 1984). Clouds have two important effects on the surface energy balance as a regulator for climate: shortwave cooling and infrared warming.

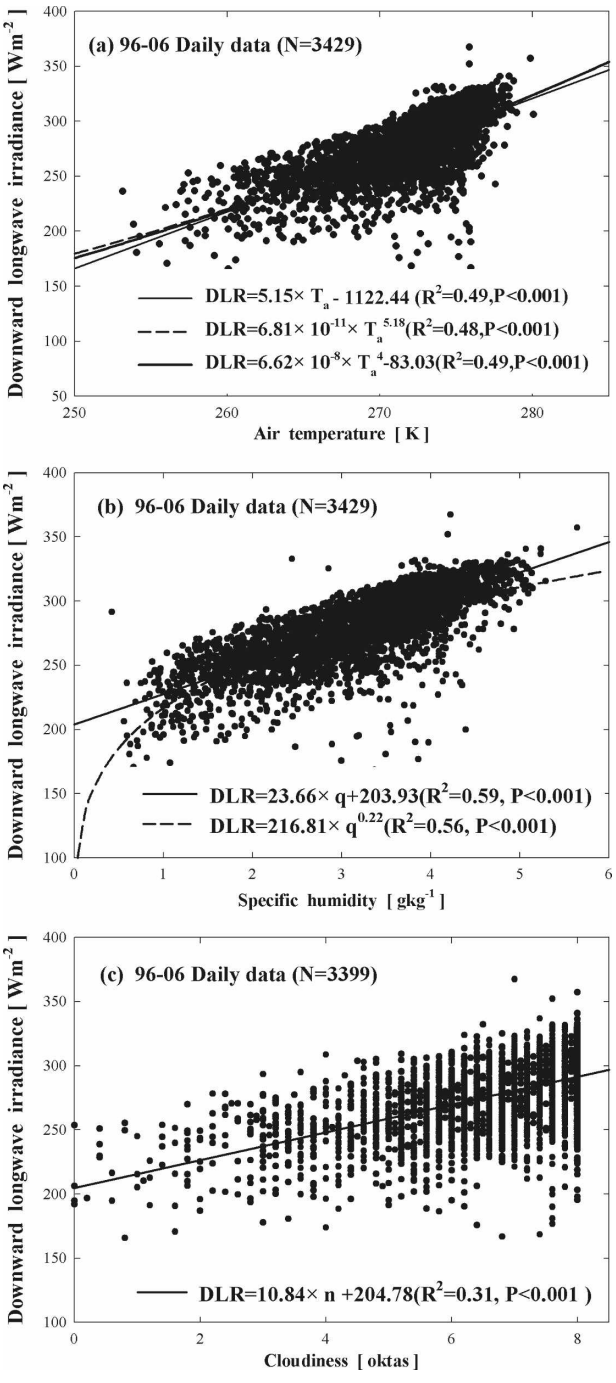

FIG. 2. Daily mean downward longwave irradiance as a function of (a) air temperature, (b) specific humidity, and (c) cloudiness for 1996–2006. Solid and dashed lines indicate the simple linear regression and power law, respectively. Number of observation data in (c) is less than in (a) and (b) because of missing cloud data.

At high latitudes, the infrared warming effect of clouds is greater than the shortwave cooling (Ramanathan et al. 1989). Air temperature is, of course, a key parameter in changes of infrared emission. Thus, the variations in

TABLE 3. Intercorrelation coefficients between daily mean downward longwave irradiance (DLR), air temperature (T_a), specific humidity (q), and cloudiness (n) at significance level $P < 0.001$.

	DLR	T_a	q	n
DLR	1.000	0.699	0.769	0.556
T_a	0.699	1.000	0.936	0.135
q	0.769	0.936	1.000	0.225
n	0.556	0.135	0.225	1.000

DLR are mainly associated with those of air temperature, water vapor, and clouds affecting the greenhouse effect.

To determine the respective relationship of air temperature (T_a), specific humidity (q), and cloudiness (n) to DLR, a simple linear regression analysis of the three variables with respect to the DLR has been carried out using the daily mean data measured at the King Sejong Station for the period from 1996 to 2006, as shown in Figs. 2a–c. Figures 2a and 2b also show the power law relationship of T_a and q to DLR, in addition to linear regression lines, and power relation where applicable.

The intercorrelation coefficients between DLR, T_a, q, and n are given in Table 3. The correlations of T_a, q, and n with DLR are 0.70, 0.77, and 0.56, respectively. It has been confirmed in Fig. 2 that daily mean DLR is all positively and significantly correlated with all three variables under all-sky conditions, with a significant level of $P < 0.001$ based on normality of the residuals and Student's t statistics for small sample sizes. Therefore, it should be noted that increases in T_a, q, and n enhance the DLR, which has a warming influence at the surface. The relations given above make it possible to determine the DLR (or $F^{\downarrow}$) from a cloudy sky using the following general equation:

$$F^{\downarrow} = f(T_a, q, n). \tag{3}$$

In a number of investigations, attempts have been made to estimate DLR empirically from the three independent variables: T_a, q, and n. In practice, empirical formulas of the Brunt and Ångström type (e.g., Kondratyev 1969) are commonly applied.

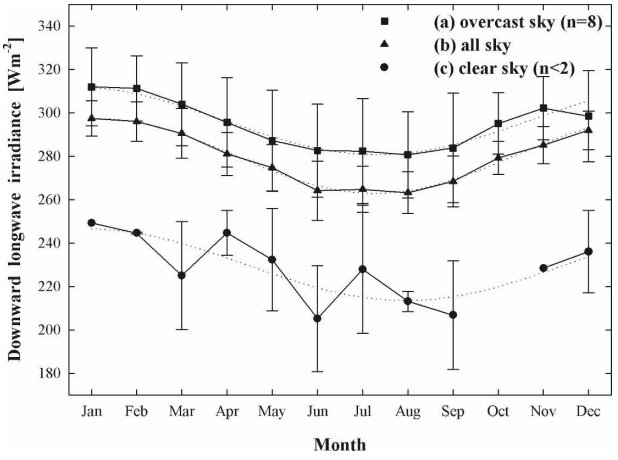

FIG. 3. Annual cycles of the DLR for (a) overcast ($n = 8$ oktas), (b) all sky (average), and (c) clear sky ($n < 2$ oktas), and their fitting curves with sine function. Vertical bar is standard deviation, and the dotted line represents the smoothed sine curves.

Figures 2a and 2b also show a power relation of T_a and q to the DLR, which are similar to the results of King (1996) for T_a and Ruckstuhl et al. (2007) for q. In addition, the regression of DLR on T_a^4 is also presented in Fig. 2a, based on the Stefan–Boltzmann law. The daily mean data used in the present analysis range from 160 to 370 W m^{-2} for DLR, from 250 to 280 K for T_a, from 0.4 to 6.0 g kg^{-1} for q, and from 0 to 8 oktas for n under all-sky conditions at the King Sejong. The best power relations obtained are DLR = $(6.81 \times 10^{-11})T_a^{5.18}$ ($R^2 = 0.48$) and DLR = $216.81q^{0.22}$ ($R^2 = 0.56$) for the daily means and DLR = $(1.02 \times 10^{-9})T_a^{4.70}$ ($R^2 = 0.75$) and DLR = $215.72\ q^{0.23}$ ($R^2 = 0.79$) for the monthly means, which are comparable to DLR = $(1.09 \times 10^{-7})T_a^{3.85}$ (King 1996) and DLR = $181.4q^{0.29}$ ($R^2 = 0.93$) for all skies (Ruckstuhl et al. 2007) in Fig. 2. From Figs. 2a and 2b the simple linear regressions expressed by a straight line are found to be about the same as the power relations in the ranges of the data, in particular. Therefore, the simple linear regressions are applied in developing the multiple linear regression model for three variables in this study.

TABLE 4. Seasonal mean DLR for clear, all, and overcast skies, and DLR cloud forcing (DLR CF). Unit: W m^{-2}.

	Clear sky		All sky		Overcast sky			
	Mean	Std	Mean	Std	Mean	Std	DLR CF	Overcast minus clear-sky DLR
Spring (SON)	209.4	23.3	277.3	11.5	291.0	15.7	68.0 (32%)	81.6 (39%)
Summer (DJF)	242.1	11.2	295.2	8.8	306.1	15.0	53.1 (22%)	64.0 (26%)
Autumn (MAM)	235.8	20.7	282.1	12.3	294.7	14.1	46.3 (20%)	58.9 (25%)
Winter (JJA)	218.3	26.8	264.0	10.9	280.8	12.9	45.7 (21%)	62.5 (29%)
Annual	228.2	12.9	279.9	6.8	293.5	8.1	51.7 (23%)	65.3 (29%)
Model [Eq. (4)] calculation	224.2		279.0		288.3		54.8 (24%)	64.0 (29%)

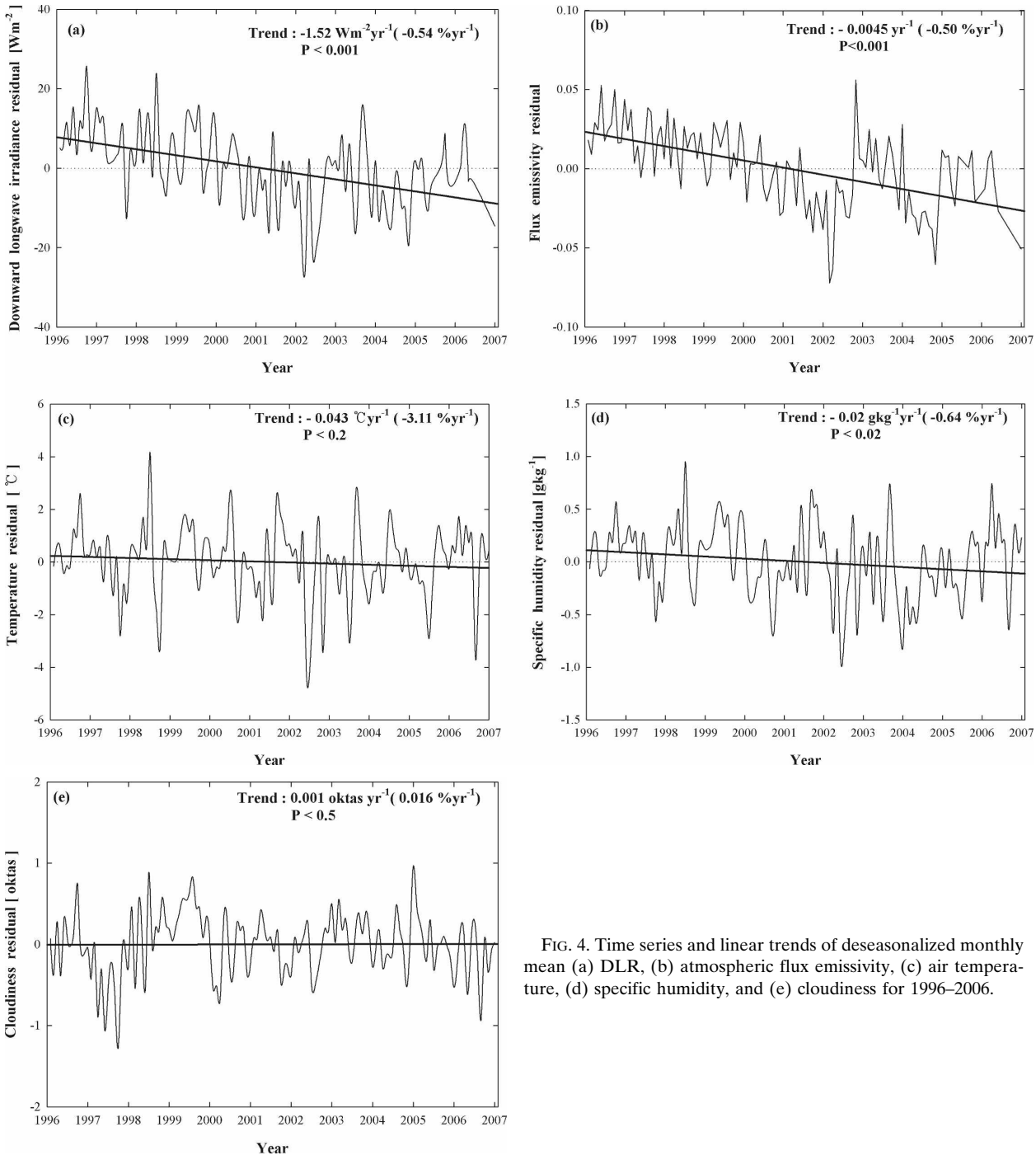

FIG. 4. Time series and linear trends of deseasonalized monthly mean (a) DLR, (b) atmospheric flux emissivity, (c) air temperature, (d) specific humidity, and (e) cloudiness for 1996–2006.

This multiple regression model can serve as the basis for testing a variety of hypotheses concerning the nature and strengths of effects of several independent variables on a quantitative dependent variable (e.g., Ezekiel and Fox 1966; Overall and Klett 1983). In this study, a multiple regression model for DLR has been developed to evaluate the effects of the three variables on the DLR using daily mean T_a, q, and n values for the period 1996–2006. The model gives the following relationship with a multiple correlation coefficient of 0.864 and a standard error of 6.89 W m^{-2} at the statistically high significance level $P < 0.001$:

$$F^{\downarrow} = 0.665T_a + 18.175q + 8.003n - 14.088. \quad (4)$$

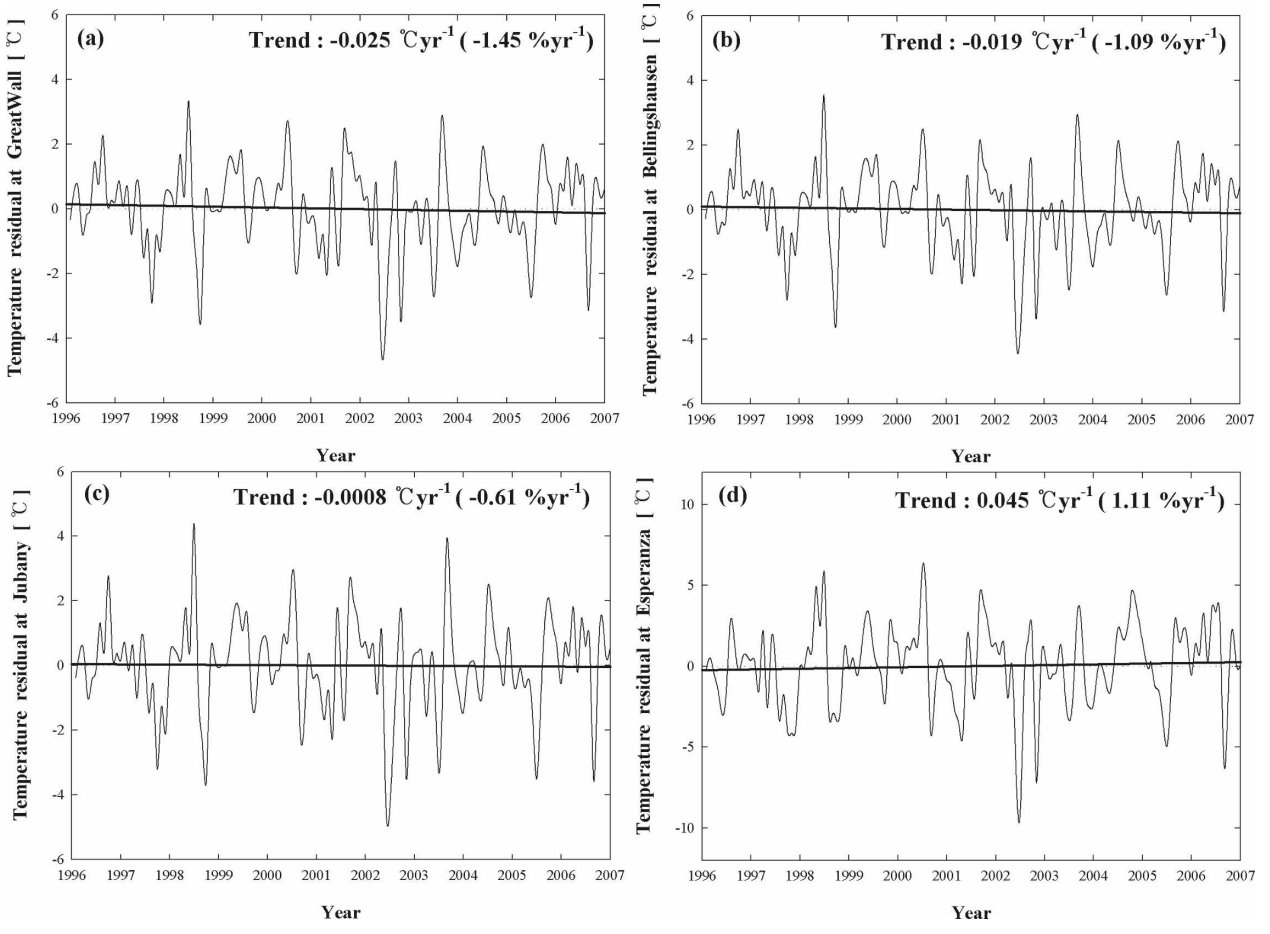

FIG. 5. Time series and linear trends of deseasonalized monthly mean air temperature for (a) Great Wall, (b) Bellingshausen, (c) Jubany, and (d) Esperanza, 1996–2006.

From the multiple regression model, the three variables T_a, q, and n together explained 75% (R^2) of all the variance in DLR under all-sky conditions. Of the 75%, the relative contribution of each individual variable to the variation of daily mean DLR has been estimated to be 6%, 46%, and 23%, respectively, using the coefficients of partial correlation (r) and the beta coefficients (β) from the statistical equation, $R^2 = \beta_2 r_{12} + \beta_3 r_{13} + \beta_4 r_{14}$ (e.g., Overall and Klett 1983). However, keeping in mind the high partial correlation ($r = 0.936$, $P < 0.001$) between the two independent variables T_a and q, as seen in Table 3, the composite contribution (52%) of them may be considered as a means of explaining the variance of DLR. Therefore, nearly all variability of the daily mean DLR is accounted for by linear regression of a composite of the two variables, that is, specific humidity and cloudiness. This leaves 25% of the variance to be explained by factors other than the three variables. On the other hand, the three variables T_a, q, and n account for 81% of the variance in the monthly mean DLR of which the contribution of n to the variation of DLR accounts for only 4% of the variations of the mean. The relatively weak dependence of DLR on n may be explained by the relatively small changes in monthly mean values, which range from about 5.5 to 8.0 oktas. Thus, using the daily mean value is more appropriate than using monthly means in the relations of T_a, q, and n with respect to DLR. Therefore, it is concluded that the use of daily mean values is reasonable for the evaluation of the individual contribution of the variables in the multiple regression analysis.

Annual cycles of the DLR for overcast ($n = 8.0$ oktas), cloudy-sky (all skies, $\bar{n} = 6.8$ oktas), and clear-sky ($n < 2.0$ oktas) conditions are shown in Fig. 3 in order to examine the effects of cloud on the DLR. Since the monthly data show periodic nature, a sine function was chosen to fit the observed data. As shown in Fig. 3, the fitted curves are almost parallel, implying that there are no remarkable seasonal variations in the differences of the DLR between the curves for overcast, cloudy, and

clear-sky conditions. This allows a simple examination of the effects of cloud on the DLR, using the differences between the fitted curves for overcast sky, cloudy sky, and clear sky. The difference between the cloudy-sky flux and clear-sky flux is defined as cloud radiative forcing (e.g., Ramanathan et al. 1989; Town et al. 2005). Thus DLR cloud forcing (DLR CF) at the surface is given by

$$\text{DLR CF} = F^{\downarrow}_{\text{all}} - F^{\downarrow}_{\text{clear}}, \tag{5}$$

where $F^{\downarrow}$ is the DLR, and the subscripts, "all" and "clear" refer to all-sky and clear-sky (cloud free) conditions. Table 4 shows the DLR CF of 52 W m^{-2} (23%) from the fact that annual mean DLR is 228 W m^{-2} for clear sky and 280 W m^{-2} for all sky, with no apparent seasonal cycle. These results agree closely with the calculations using the multiple regression model [Eq. (4)], which are 55 W m^{-2} (24%) in DLR CF, as listed in the last row of Table 4. It is therefore suggested that in further studies the multiple regression model be applied to estimate the radiative forcings for those major variables that influence DLR variability. Further, the all-sky DLR CF compares closely with the 46 W m^{-2}, the difference between cloudy-sky flux (324 W m^{-2}) and clear-sky flux (278 W m^{-2}) at the surface, as presented in the earth's annual global mean energy budget (Kiehl and Trenberth 1997). At the South Pole, the annual DLR CRF for 2001 was about 23 W m^{-2} for annual-mean fractional cloud cover (FCC) of 60% (Town et al. 2005). This DLR CF is less than half of the King Sejong's DLR CF owing to higher values in temperature (−1.4°C), FCC (85%), and cloud optical depth at King Sejong based on Moderate Resolution Imaging Spectroradiometer (MODIS) data.

Furthermore, it is interesting to investigate the difference between overcast-sky flux and clear-sky value. Overcast clouds give an increase of 65 W m^{-2} (29%) in the annual mean difference between the overcast and the clear-sky flux as seen in the second row from the bottom of Table 4. Yamanouchi and Kawaguchi (1984) reported that clouds are most effective in increasing the DLR, by 80 W m^{-2} comparing clear to overcast (middle or low clouds) sky throughout the year (1979–81). They found that the effect of clouds on DLR does not vary significantly with the season at Mizuho Station (70.41°S, 44.20°E) in Antarctica. According to the data by Boltz (Kondratyev 1969), the DLR of a cloudy-sky flux exceeds that of a cloudless sky by 22% in Germany, which is in good agreement with the 23% in this study. In summary, results similar to those of the present study have been obtained in previous studies (Kiehl and Trenberth 1997; Yamanouchi and Kawaguchi 1984; Kondratyev 1969) even though the location and period are different.

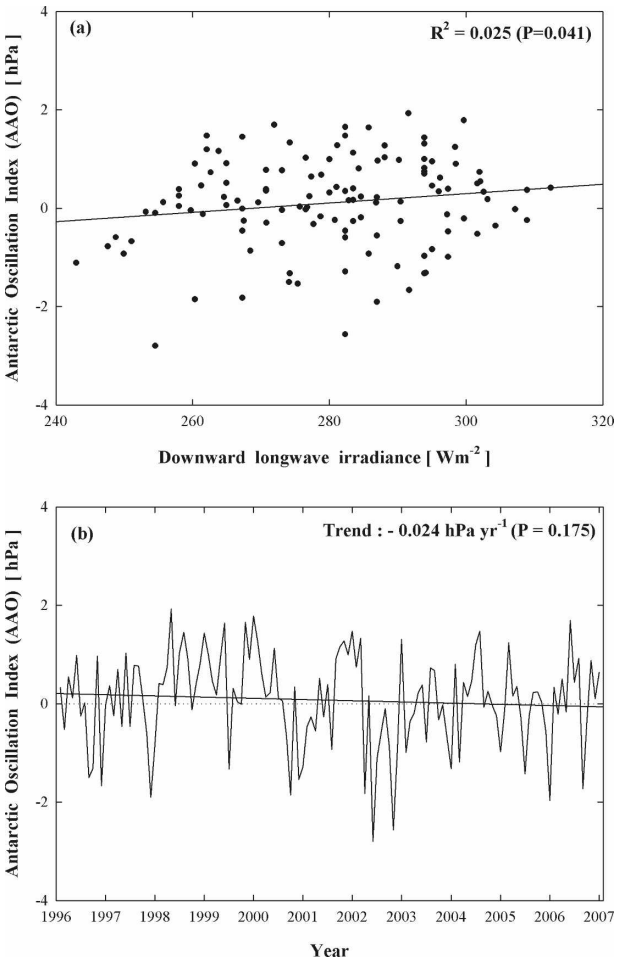

FIG. 6. (a) Relationship between DLR and the AAO at the significance level $P < 0.05$, and (b) the AAO trend at $P = 0.175$.

b. Trends

A linear regression analysis of the respective DLR ($F^{\downarrow}$), atmospheric flux emissivity (ϵ^f), air temperature (T_a), specific humidity (q), and cloudiness (n) has been carried out to evaluate trends, that is, the slope of linear regressions, from the time series of the deseasonalized monthly mean values for the 11 years (1996–2006). The deseasonalized values (residuals) are calculated with respect to 1996–2006 climatological seasonal means. Time series and linear trends for $F^{\downarrow}$, ϵ^f, T_a, q, and n are represented in Fig. 4. As shown in Figs. 4a and 4b, the annual mean trend in $F^{\downarrow}$ and ϵ^f represents statistically highly significant decreases of -1.52 ± 0.26 W m^{-2} yr^{-1} ($-0.54 \pm 0.09\%$ yr^{-1}) and -0.005 ± 0.0006 yr^{-1} ($-0.50 \pm 0.07\%$ yr^{-1}), respectively, at the $P < 0.001$ significance level. From the trends presented in Figs. 4c

TABLE 5. Monthly linear trends and statistics of DLR, air temperature, specific humidity, and cloudiness, 1996–2006: mean significance level (SL), standard deviation (Std), and standard error (SE).

	Jan	Feb	Mar	Apr	May	Jun	Jul	Aug	Sep	Oct	Nov	Dec	Year
(a) DLR (W m^{-2})													
Slope (W m^{-2} yr^{-1})	−1.38	−0.71	−1.54	−1.63	−1.90	−3.12	−2.50	−0.78	−0.30	−1.80	−2.00	−1.75	−1.52
SL	0.04	0.23	0.08	0.04	0.03	0.04	0.03	0.25	0.42	0.01	0.03	0.03	0.00
Mean value	297.4	296.0	290.5	281.1	274.7	264.1	264.8	263.3	268.4	279.3	285.1	291.9	279.9
Std	8.2	9.1	11.4	9.9	10.7	13.6	10.6	9.6	11.7	7.6	8.6	8.9	6.8
SE	2.5	2.8	3.4	3.0	3.2	4.5	3.5	3.0	3.7	2.4	2.9	2.8	2.3
(b) Air temperature (°C)													
Slope (°C yr^{-1})	−0.04	−0.03	−0.04	−0.08	−0.12	−0.19	−0.01	−0.05	0.18	0.02	0.02	−0.02	−0.04
SL	0.23	0.30	0.32	0.27	0.23	0.25	0.48	0.41	0.18	0.45	0.39	0.42	0.15
Mean value	2.2	2.1	1.0	−0.6	−2.0	−4.6	−4.7	−4.6	−4.0	−1.8	−0.4	0.9	−1.4
Std	0.5	0.5	0.9	1.2	1.6	2.6	1.3	1.9	2.0	1.3	0.7	0.7	0.5
SE	0.2	0.2	0.3	0.4	0.5	0.8	0.4	0.6	0.6	0.4	0.2	0.2	0.1
(c) Specific humidity (g kg^{-1})													
Slope (g kg^{-1} yr^{-1})	−0.03	−0.02	−0.03	−0.02	−0.03	−0.06	−0.02	−0.01	0.02	0.001	0.01	−0.03	−0.02
SL	0.09	0.23	0.24	0.25	0.27	0.10	0.22	0.40	0.32	0.49	0.34	0.18	0.03
Mean value	4.0	4.0	3.7	3.3	3.0	2.4	2.4	2.5	2.6	3.1	3.3	3.6	3.2
Std	0.2	0.3	0.4	0.3	0.4	0.5	0.2	0.4	0.4	0.4	0.3	0.3	0.2
SE	0.1	0.1	0.1	0.1	0.1	0.1	0.1	0.1	0.1	0.1	0.1	0.1	0.1
(d) Cloudiness (oktas)													
Slope (oktas yr^{-1})	0.01	0.06	0.01	−0.02	0.04	−0.02	−0.001	−0.04	0.01	−0.02	0.002	0.02	0.001
SL	0.37	0.03	0.46	0.32	0.21	0.35	0.49	0.20	0.45	0.31	0.47	0.35	0.37
Mean value	6.8	7.0	6.9	6.8	6.7	6.7	6.8	6.8	6.9	6.8	6.9	6.9	6.8
Std	0.3	0.3	0.5	0.4	0.5	0.5	0.4	0.4	0.5	0.3	0.2	0.4	0.4
SE	0.1	0.1	0.1	0.1	0.1	0.1	0.1	0.1	0.2	0.1	0.1	0.1	0.1

and 4d, the annual mean T_a and q also have decreased at a rate of -0.04 ± 0.04°C yr^{-1} ($-3.11 \pm 2.70\%$ yr^{-1}, $P < 0.20$) and -0.02 ± 0.01 g kg^{-1} yr^{-1} ($-0.64 \pm 0.30\%$ yr^{-1}, $P < 0.02$), respectively, while the n showed an insignificantly increasing tendency, 0.001 ± 0.01 oktas yr^{-1} ($0.02 \pm 0.16\%$ yr^{-1}, $P < 0.50$) in Fig. 4e. This increasing trend in n during the last decade is consistent with the observed reduction (-0.24 Wm^{-2} yr^{-1} or -0.29% yr^{-1}) in surface solar irradiance (not shown here).

To see the consistency of the results at the King Sejong Station (62°13′S, 58°57′W), the trends for air temperature at the five neighboring stations of Bellingshausen (62°11′S, 58°57′W), Great Wall (62°12′S, 58°47′W), Jubany (62°14′S, 58°40′W), Esperanza (63°23′S, 56°59′W), and Marambio (62°15′S, 56°39′W) covering 60~65°S, 55~60°W have been analyzed. Air temperature data is taken from the British Antarctic Survey (BAS) Web site (http://www.nerc-bas.ac.uk/icd/gjma/temps.html), for the same period (1996–2006). Figure 5 shows cooling trends at three stations located on King George Island (-0.019°C yr^{-1} for Bellingshausen, -0.025°C yr^{-1} for Great Wall, and -0.0008°C yr^{-1} for Jubany) that are similar to those found at King Sejong Station (-0.043°C yr^{-1}). The other two stations located at higher latitudes and relatively far from the King George Island showed warming trends over the same period (0.045°C yr^{-1} for Esperanza and 0.088°C yr^{-1} for Marambio, not shown here). For the longer term 1988–2006, warming trends appear at all six stations: 0.027°C yr^{-1} for King Sejong, 0.037°C yr^{-1} for Bellingshausen, 0.032°C yr^{-1} for Great Wall, 0.044°C yr^{-1} for Jubany, 0.088°C yr^{-1} for Esperanza, and 0.10°C yr^{-1} for Marambio. Thus, it is found that there is strong consistency between King Sejong and its near neighbors in the temperature trend. Although the last decade showed a cooling trend at King Sejong Station together with neighboring stations in King George Island, the longer period has exhibited warming trends at most stations on the Antarctic Peninsula including King Sejong (cf. BAS Web site; Hodgson et al. 2006).

Since the variation in DLR is closely related to the variation of T_a, q, and n, as elucidated in the previous section, it may be concluded that the recent decadal decrease in DLR is attributed mainly to the net decrease of T_a and q after compensating the increased effect of n at the King Sejong Station. Lee et al. (2003) showed that the variations in T_a at King Sejong and around the Antarctic Peninsula are closely associated with the regional atmospheric circulation. Wallace and Thompson (2002) found that the trend of the Antarctic Oscillation (AAO) has been positive over the last decade with stronger westerly flow encircling the polar cap, substantially contributing to the observed warming

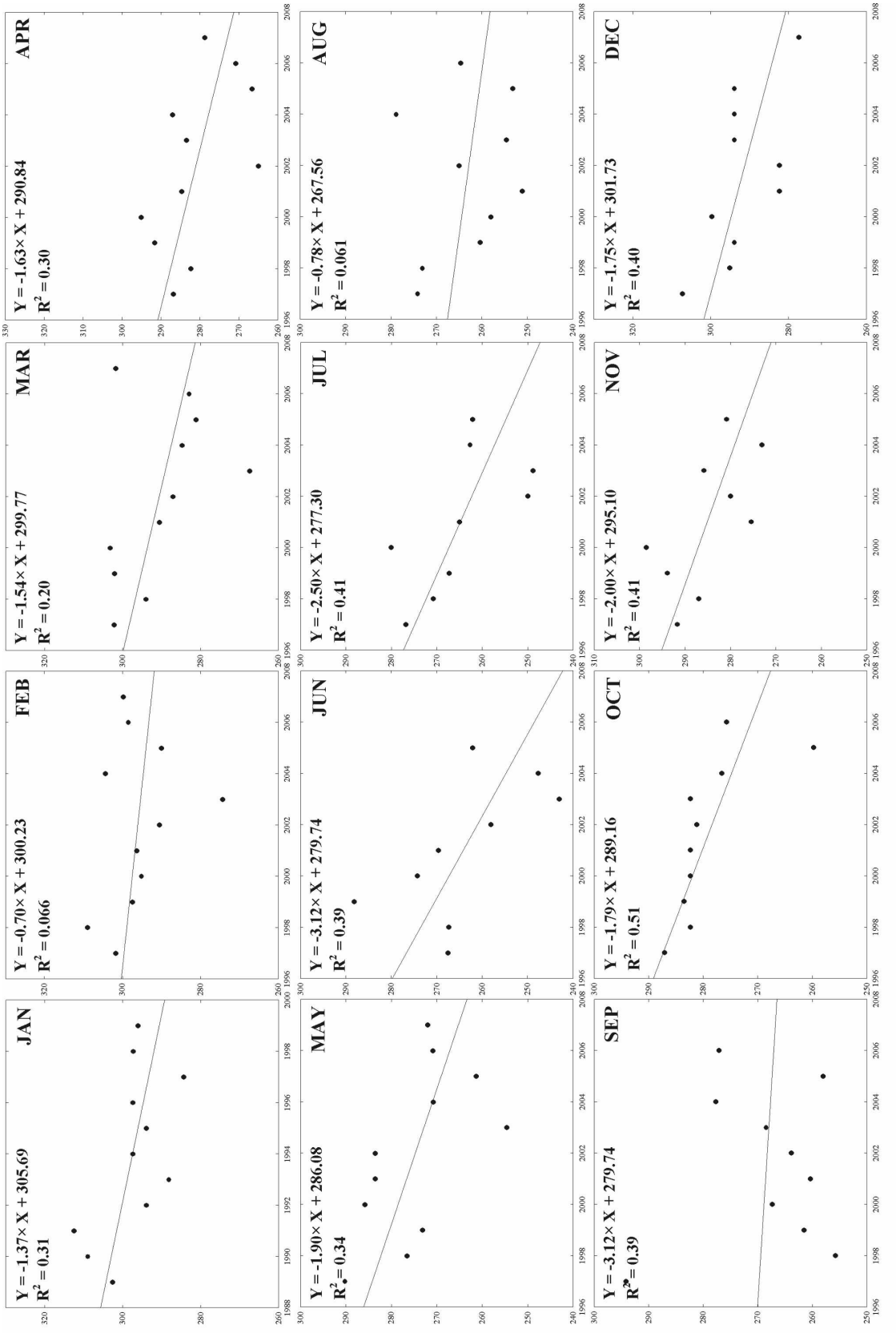

FIG. 7. As in Fig. 4 except for monthly mean DLR, 1996–2006. One time series is plotted for each month. Note that each month is scaled differently according to the range in the data. See Table 5 for statistics.

over the Antarctic Peninsula and Patagonia and to cooling over the eastern Antarctic. To show the relationship between AAO and DLR, a simple linear regression analysis of the DLR with the AAO has been also carried out using the monthly mean data. (The AAO data calculated from the monthly mean 700-hPa height anomalies poleward of 20° latitude for the Southern Hemisphere are available online at http://www.cpc.ncep.noaa.gov/products/precip/CWlink/daily_ao_index/aao/aao_index.html.) The DLR is positively correlated with the AAO at significance level $P < 0.05$, as shown in Fig. 6a. The AAO trend shows an insignificant decrease of 0.024 hPa yr^{-1} over the period 1996–2006, as shown in Fig. 6b, but for the longer period, 1988–2006, the trend of AAO follows increasing trends of T_a and q, as noted in the previous paragraph. As a result, it is likely that variations of DLR are also clearly related to behavior of the AAO in connection with polar circulation. To gain a comprehensive understanding of the influence of the AAO on DLR, further studies are needed concerning the relationship between DLR and the AAO.

To examine individual trends by months, linear regression analyses are also carried out as for annual trends. The results are given in Table 5. We also plotted the monthly mean DLR for each month in Fig. 7. As seen in Table 5a and Fig. 7, the DLR shows decreasing tendencies for all months through the year. Particularly, except for the four months of February, March, August, and December, the decreases in DLR are significant at the $P < 0.05$ significance level. Both air temperature and specific humidity (Tables 5b and 5c) show insignificant decreasing trends for all months except for the spring months (September–November). Cloudiness (Table 5d) shows a positive trend for summer months and a negative trend for winter months. Consequently, as for annual trends, monthly mean trends show that, as a whole, the changes in DLR are associated with T_a, q, and n, despite the fact that it is difficult to explain the statistically insignificant trends in the late winter months.

5. Summary and conclusions

Effects of air temperature, specific humidity, and cloudiness on the variation of downward longwave irradiance and their long-term trends have been examined using the daily and monthly mean values measured at King Sejong Station over the period from 1996 to 2006.

It has been shown that the downward longwave irradiance (DLR) is positively correlated with three variables: air temperature, specific humidity, and cloudiness—all of which have statistically high significance. A multiple linear regression model for DLR using daily data for the three variables has been developed to evaluate their effects on DLR. The three variables together explained 75% of the variance in daily mean DLR. While cloudiness contributes 23% to the variation in DLR, nearly all DLR variability is accounted for by the variations in specific humidity and cloudiness taken together. The annual mean of DLR cloud forcing at the surface is 52 W m^{-2} (23%) with no remarkable seasonal cycle, and the overcast-sky flux give also an increase of 65 W m^{-2} (29%) from clear-sky value throughout the year. It is suggested that the multiple regression model can be used to estimate the radiative forcing as a function of the variables, giving the influence on the DLR variability through further studies.

The annual mean trend in DLR shows a statistically significant decrease of -1.52 W m^{-2} yr^{-1} (-0.54% yr^{-1}) in the time series of monthly mean values. Accordingly, the flux emissivity, air temperature, and specific humidity have also decreased in their time series, while cloudiness has increased insignificantly. Thus, it can be concluded that the recent decrease in DLR is caused by the net cooling effect due to air temperature and specific humidity, after offsetting for the slight warming effect of cloudiness. Analysis of mean monthly trends for individual months shows that, as for the annual data, the variations in DLR are mostly associated with variations of air temperature, specific humidity, and cloudiness.

Acknowledgments. This work was partially supported by KOPRI's COMPAC project and by the Second Phase Brain Korea 21 Research Program 2006.

REFERENCES

Alados-Arboledas, L., J. Vida, and J. I. Jiménez, 1988: Effects of solar radiation on the performance of pyrgeometers with silicon domes. *J. Atmos. Oceanic Technol.,* **5,** 666–670.

Dutton, E. G., R. S. Stone, D. W. Nelson, and B. G. Mendonca, 1991: Recent interannual variations in solar radiation, cloudiness, and surface temperature at the South Pole. *J. Climate,* **4,** 848–858.

Eppley, 2006: Precision Infrared Radiometer, Mode PIR Instruction sheet. The Eppley Laboratory, 4 pp.

Ezekiel, M., and K. A. Fox, 1966: *Method of Correlation and Regression Analysis.* John Wiley and Sons, 548 pp.

Fairall, C. W., P. O. G. Persson, E. F. Bradley, R. E. Payne, and S. A. Anderson, 1998: A new look at calibration and use of Eppley Precision Infrared Radiometers. Part I: Theory and application. *J. Atmos. Oceanic Technol.,* **15,** 1229–1242.

Goody, R. M., and Y. L. Yung, 1989: *Atmospheric Radiation: Theoretical Basis.* Oxford University Press, 519 pp.

Hodgson, D., M. J. Bentley, S. J. Roberts, J. A. Smith, D. E. Sugden, and E. W. Domack, 2006: Examining Holocene stability

of Antarctic Peninsula ice shelves. *Eos, Trans. Amer. Geophys. Union,* **87,** 305, doi:10.1029/2006EO310001.

Kiehl, J. T., and K. E. Trenberth, 1997: Earth's annual global mean energy budget. *Bull. Amer. Meteor. Soc.,* **78,** 197–208.

Kim, J., H. K. Cho, Y. Jung, Y. G. Lee, and B. Y. Lee, 2006: Surface energy balance at Sejong Station, King George Island, Antarctica. *Atmosphere,* **16,** 111–124.

King, J. C., 1994: Recent climate variability in the vicinity of the Antarctic Peninsula. *Int. J. Climatol.,* **14,** 357–369.

——, 1996: Longwave atmospheric radiation over Antarctica. *Antarct. Sci.,* **8,** 105–109.

——, P. S. Anderson, M. C. Smith, and S. D. Mobbs, 1996: The surface energy and mass balance at Halley, Antarctica during winter. *J. Geophys. Res.,* **101,** 19 119–19 128.

Kondratyev, K. Ya., 1969: *Radiation in the Atmosphere.* Academic Press, 912 pp.

Lee, B. Y., T.-Y. Kwon, J.-S. Lee, and Y. I. Won, 2002: Surface air temperature variations around the Antarctic Peninsula: Comparison of the west and east sides of the Peninsula. *Ocean Polar Res.,* **24,** 267–278.

Lee, J.-S., T.-Y. Kwon, B. Y. Lee, H. I. Yoon, and J. W. Kim, 2003: Change of regional atmospheric circulation related with recent warming in the Antarctic Peninsula. *Ocean Polar Res.,* **25,** 503–518.

Liou, K. N., 2002: *An Introduction to Atmospheric Radiation*. Academic Press, 583 pp.

Overall, J. E., and C. J. Klett, 1983: *Applied Multivariate Analysis*. R. E. Krieger, 500 pp.

Philipona, R., and Coauthors, 2001: Atmospheric longwave irradiance uncertainty: Pyrgeometers compared to an absolute sky-scanning radiometer, atmospheric emitted radiance interferometer, and radiative transfer model calculations. *J. Geophys. Res.,* **106,** 28 129–28 142.

Ramanathan, V., R. D. Cess, E. F. Harrison, P. Minnis, B. R. Barkstrom, E. Ahmad, and D. Hartman, 1989: Cloud radiative forcing and climate: Results from the earth radiation budget experiment. *Science,* **243,** 57–63.

Reijmer, C. H., and J. Oerlemans, 2002: Temporal and spatial variability of the surface energy balance in Dronning Maud Land, East Antarctica. *J. Geophys. Res.,* **107,** 4759, doi:10.1029/2000JD000110.

Ruckstuhl, C., R. Philipona, J. Morland, and A. Ohmura, 2007: Observed relationship between surface specific humidity, integrated water vapor, and longwave downward radiation at different altitudes. *J. Geophys. Res.,* **112,** D03302, doi:10.1029/2006JD007850.

Schlatter, T. W., 1972: The local surface energy balance and surface temperature region in Antarctica. *J. Appl. Meteor.,* **11,** 1048–1062.

Stanhill, G., and S. Cohen, 1997: Recent changes in solar irradiance in Antarctica. *J. Climate,* **10,** 2078–2086.

Studinger, M., D. Bromwich, B. Csatho, R. Muench, T. Parish, and J. Stith, 2005: Science opportunities for a long-range Antarctic research aircraft. *Eos, Trans. Amer. Geophys. Union,* **86,** 39, doi:10.1029/2005EO040004.

Town, M. S., V. P. Walden, and S. G. Warren, 2005: Spectral and broadband longwave downwelling radiative fluxes, cloud radiative forcing, and fractional cloud cover over the South Pole. *J. Climate,* **18,** 4235–4252.

Ueno, T., S. Shibata, Y. Irose, and T. Okamoto, 2000: On the pyrgeometers with a shadow disk. *J. Aerol. Obs.,* **60,** 35–38.

Van den Broeke, M., C. Reijmer, and R. van de Wal, 2004: Surface radiation balance Antarctica as measured with automatic weather stations. *J. Geophys. Res.,* **109,** D09103, doi:10.1029/2003JD004394.

Vaughan, D. G., and C. S. M. Doake, 1996: Recent atmospheric warming and retreat of ice shelves on the Antarctic Peninsula. *Nature,* **79,** 328–331.

Wallace, J. M., and D. W. J. Thompson, 2002: The Pacific center of action of the Northern Hemisphere annular mode: Real or artifact? *J. Climate,* **15,** 1987–1991.

WMO, 2007: Polar meteorology: Understanding global impacts. WMO 1013, 38 pp.

Yamanouchi, T., and S. Kawaguchi, 1984: Longwave radiation balance under a strong surface inversion in the katabatic wind zone, Antarctica. *J. Geophys. Res.,* **89,** 11 771–11 778.